Available online at www.sciencedirect.com
ScienceDirect
Biomaterials 28 (2007) 671–679
Biomaterials
www.elsevier.com/locate/biomaterials

Cell adaptation to a physiologically relevant ECM mimic with different viscoelastic properties

Kaustabh Ghosh[a], Zhi Pan[b], E Guan[b], Shouren Ge[b], Yajie Liu[c], Toshio Nakamura[c], Xiang-Dong Ren[d,e], Miriam Rafailovich[b], Richard A.F. Clark[a,d,f,*]

[a]Department of Biomedical Engineering, SUNY at Stony Brook, Stony Brook, New York 11794, USA
[b]Department of Material Science and Engineering, SUNY at Stony Brook, Stony Brook, New York 11794, USA
[c]Department of Mechanical Engineering, SUNY at Stony Brook, Stony Brook, New York 11794, USA
[d]Department of Dermatology, SUNY at Stony Brook, Stony Brook, New York 11794, USA
[e]Department of Pharmacology, SUNY at Stony Brook, Stony Brook, New York 11794, USA
[f]Department of Medicine, SUNY at Stony Brook, Stony Brook, New York 11794, USA

Received 15 July 2006; accepted 27 September 2006
Available online 17 October 2006

Abstract

To successfully induce tissue repair or regeneration in vivo, bioengineered constructs must possess both optimal bioactivity and mechanical strength. This is because cell interaction with the extracellular matrix (ECM) produces two different but concurrent signaling mechanisms: ligation-induced signaling, which depends on ECM biological stimuli, and traction-induced signaling, which depends on ECM mechanical stimuli. In this report, we provide a fundamental understanding of how alterations in mechanical stimuli alone, produced by varying the viscoelastic properties of our bioengineered construct, modulate phenotypic behavior at the whole-cell level. Using a physiologically relevant ECM mimic composed of hyaluronan and fibronectin, we found that adult human dermal fibroblasts modify their mechanical response in order to match substrate stiffness. More specifically, the cells on stiffer substrates had higher modulus and a more stretched and organized actin cytoskeleton (and vice versa), which translated into larger traction forces exerted on the substrate. This modulation of cellular mechanics had contrasting effects on migration and proliferation, where cells migrated faster on softer substrates while proliferating preferentially on the stiffer ones. These findings implicate substrate rigidity as a critical design parameter in the development of bioengineered constructs aimed at eliciting maximal cell and tissue function.

Keywords: Dermal fibroblasts; Cell mechanics; Hydrogel stiffness; Hyaluronan; Fibronectin

1. Introduction

To effectively repair, regenerate or engineer tissues, bioactive constructs must be created that are able to promote adhesion, migration, proliferation and differentiation of cells appropriate to the particular tissues [1]. Recently, it has been shown that substrate mechanics can modulate tissue cell phenotype in a way similar to biochemical signals [2,3]. These studies have been performed on a variety of substrates, more commonly on the collagen-coated silicone or polyacrylamide gels [4–6]. However, to fully understand cell functional responses in the context of a specific tissue, it is important to create an environment that very closely mimics the actual in vivo conditions. This necessitates the development of physiologically relevant, tissue-engineered constructs that resemble native tissue and whose mechanical properties can be strictly controlled to allow the evaluation of structure–function relationship at the cell/biomaterial interface.

To this end, we have recently developed a tissue-engineered construct composed of hyaluronan (HA) and fibronectin (FN) functional domains [7]. Importantly, both HA and FN are

*Corresponding author. Department of Biomedical Engineering, Dermatology and Medicine, HSC, T-16, Rm 60, SUNY at Stony Brook, Stony Brook, NY 11794 8165, USA. Tel.: +1 631 444 7519; fax: +1 631 444 3844.
E-mail address: rclark@notes.cc.sunysb.edu (R.A.F. Clark).

0142-9612/$ - see front matter © 2006 Elsevier Ltd. All rights reserved.
doi:10.1016/j.biomaterials.2006.09.038

important components of the ECM at times of cell migration and tissue organization during tissue repair, embryogenesis and morphogenesis [8]. Therefore, in contrast to the protein-coated silicone or polyacrylamide gels, our hydrogel provides a physiological setting for the evaluation of cell functional responses. Furthermore, we have previously shown that the mechanics (shear modulus, G') of these hydrogels can be precisely controlled by altering the crosslinker bulk density [9]. In addition, since in these hydrogels, the molar ratios of FN domains to crosslinker are extremely small, variation in ligand bulk density would have no significant impact on crosslinker bulk density. Thus, our hydrogel construct provides a single system in which both substrate mechanics (a function of crosslinker bulk density) and biochemical signaling (a function of ligand type and bulk density) can be independently altered and their effect on cell genotype and phenotype monitored. This study discusses alterations in only substrate mechanical properties while variations in ligand type and bulk density and its effect on cell function is currently being investigated and will be reported separately.

An important application of these hydrogel constructs is to accentuate the repair of acute and chronic cutaneous wounds. Dermal fibroblasts are the primary cells involved in cutaneous reparative process. Therefore, in this study, we investigated the mechanisms with which adult human dermal fibroblasts (AHDFs) sense and respond to hydrogel mechanics to ultimately affect function at the whole cell level. Hydrogels were prepared with different crosslinking densities to provide levels of stiffness that varied by at least half order of magnitude [9]. We first measured the modulus of live AHDFs to determine whether cell stiffness was altered to adapt to substrate mechanics. Next, we visualized the cellular F-actin fibers to determine whether there were any cytoskeleton changes responsible for the observed differences in cell stiffness. It is known that intracellularly generated contractile forces are transmitted to the cell–substrate adhesive complexes (focal adhesions) via actin cytoskeleton and exerted on the substrate as traction [10]. Therefore, using digital image speckle correlation (DISC) technique [11] in combination with finite element method (FEM), we determined whether the traction forces exerted by cell on the substrate were also affected by substrate mechanics. Since cell migration and proliferation are critical functions involved during tissue repair that involve cellular tractional forces, we also determined whether fibroblast migration and proliferation were also affected in a manner similar to that observed for cellular traction. In this manner, we were able to obtain a comprehensive picture of the structure–function relationship at the cell/material interface.

2. Materials and methods

2.1. Preparation of hydrogel substrates

Hydrogel substrates were synthesized as reported previously [7,9]. Briefly, the fibronectin functional domains (FNfds) were coupled to the crosslinker poly(ethylene glycol) diacrylate (PEGDA) (Nektar Therapeutics, Huntsville, AL) to form PEGDA-FNfd conjugates (in PBS). These conjugates were then mixed with excess PEGDA and thiol-functionalized HA (HA-DTPH) in serum free-DMEM (SF-DMEM, Sigma, St. Louis, MO) to obtain bioactive hydrogels that were plated in 35-mm tissue culture dishes. Final concentration of HA-DTPH in the hydrogels was always 1% (w/v). The stiffness of these hydrogels was modulated by altering the crosslinker concentration. PEGDA solutions of 4.5%, 1.5% and 0.75% (w/v) resulted in shear storage moduli of 4270 Pa, 550 and 95 Pa, respectively, as measured by oscillatory shear rheometry [9]. Irrespective of the stiffness, the biochemical signaling was maintained constant by using all three FNfds at the optimal bulk density of 0.26 μM [7]. Post-gelation, all hydrogels were cured for 24 h to stabilize PEGDA-mediated crosslinking [9].

2.2. Cell culture

Primary adult human dermal fibroblasts (AHDFs) were obtained from Clonetics, San Diego, CA and used between passages 5 and 13. The cells were routinely cultured in DMEM supplemented with 10% fetal bovine serum (HyClone, Logan, UT) and an antibiotic mix of penicillin, streptomycin and L-Glutamine (FULL-DMEM), in a 37 °C, 5% CO_2, 95% humidity incubator (Napco Scientific Company, Tualatin, OR). Regardless of the functional assay, the AHDF monolayers were grown to nearly 80% confluence, harvested, then centrifuged to obtain a pellet that was rinsed twice with SF-DMEM + 2% bovine serum albumin (fraction V, MP Biomedicals, Irvine, CA), and finally resuspended in SF-DMEM or FULL-DMEM for use in functional assays.

2.3. Cell stiffness

Cell stiffness was measured using an atomic force microscope (AFM, Dimension 3000; Digital Instruments, Co., Ltd. Santa Barbara, CA), which was operated in shear modulation force microscopy (SMFM) mode [12] using a silicon nitride tip on a cantilever with a bending spring constant of 0.06 N/m. AHDFs were seeded on hydrogels of different stiffness at 500 cells/cm^2 and incubated for 12 h at 37 °C prior to measurement. During the measurement, a force of ~2 nN was exerted by the cantilever on the cell's perinuclear region and a sinusoidal drive signal (1400 Hz) was applied to the x-piezo controlling cantilever, inducing a small oscillatory motion of the tip parallel to the cell surface. When the drive signal amplitude was varied from 7.5 mV up to 125 mV, which corresponds to an x-piezo displacement of 1.5–25 nm, the cantilever response was recorded to estimate the stiffness of the cell surface [13]. The AFM set-up was calibrated such that a greater response amplitude indicated a more compliant surface and vice versa. The drive frequency of 1400 Hz was chosen for the measurements since it lies in the flattest region of the cantilever's response curve. A total of nine experimental points (three points per cell and three cells per sample) were obtained for each hydrogel condition.

2.4. Cellular actin cytoskeleton organization

AHDFs were seeded on hydrogels of different stiffness at 500 cells/cm^2 and incubated for 12 h at 37 °C. The choice of this incubation time was based on the observation that AHDF spread maximally between 6–12 h post-seeding. To determine actin cytoskeleton organization, the cells were fixed with 3.7% (w/v) formaldehyde, permeabilized with a mild detergent (1% Nonidet P-40, Sigma), stained with Alexa Fluor-488 Phalloidin (Molecular Probes, Eugene, OR) and imaged using a Leica TCS SP2 laser scanning confocal microscope (Leica microsystem Inc., Bannockburn, IL).

2.5. Cellular traction forces and mechanical work using DISC and FEA

The traction forces exerted by cells on the substrate were measured using Digital Image Speckle Correlation (DISC) [11], coupled with finite

element analysis (FEA) modeling [14]. Fluorescent beads (40 nm diameter, Molecular Probes, Eugene, OR) were sonicated and suspended at a concentration of 5% (v/v) in the HA solution prior to gelation to obtain uniform dispersion. This concentration was chosen in order to achieve a high density of speckles for the DISC technique, while at the same time remaining sufficiently dilute to prevent clustering. The HA solution was then crosslinked using PEGDA. Post-gelation, the hydrogels were cured at 4 °C for 18 h to stabilize PEGDA-mediated crosslinking. AHDFs were then seeded on the different hydrogels at 500 cells/cm^2, which was a sufficiently low density to obtain single cells per high power view, and cultured for ~6 h at 37 °C. The location of single cells attached to the surface was determined by a differential interference contrast (DIC) lens, and the distribution of embedded fluorescent beads beneath the cells and in the surrounding region was simultaneously recorded using a 63×, aperture 0.9 water objective lens on a Leica TC S SP2 laser scanning confocal microscope (Leica microsystem Inc., Bannockburn, IL). At least 4 cells were evaluated for each hydrogel condition, the sample size being chosen based on the variation obtained. To obtain maximal resolution in the z-direciton, the pinhole size was automatically adjusted by the Leica software. This ensured that only the beads in this top narrow layer of the substrate were recorded. EDTA (GibcoBRL/Life Technologies, Grand Island, NY) was then added to the medium that causes cell detachment and the bead locations were recorded again using a CCD camera. The DISC technique was then used to compare the distribution of all beads (speckles) between the original and final images, and produce a vector displacement map of the substrate surface corresponding to the cell-induced deformation.

2.5.1. FEA

For computational purposes, the hydrogel substrate was modeled as a long vertical beam with a surface area of $209 \times 209\,\mu m^2$. The height of substrate was set at 418 μm since the cell-induced deformations were negligible along the z-direction and displacement field was assumed to be localized on the substrate surface ($h = 0$). This displacement field generated by DISC was used to calculate the shear stress distribution. In this FEA model, 8281 (91×91) displacement vectors, evenly distributed across the surface of the substrate, were generated and corresponding nodes to each measurement point on substrate surface were created. 8-node linear brick elements were selected and a total of 91,091 nodes and 81,000 elements were created in this 3-D model.

The hydrogel was assumed to be a homogenous, isotropic, and linearly elastic material whose mechanical properties can be expressed by two independent variables viz. Young's modulus (E) and Poisson's ratio (v). E was obtained from the relation $E = 2(1 + v)G$, with the shear modulus (G) of the hydrogels known [9] and a Poisson's ratio of 0.49 chosen due to the incompressible nature of hydrogels. The calculation of cellular shear stress was then based on the linear elastic theory [15].

If the substrate deformation is assumed to be elastic, the entire work performed by the cellular traction forces (W) will be stored in the substrate in the form of strain energy (E), where

$$W = E = \frac{1}{2}\int \sigma_{ij}(\vec{r})\varepsilon_{ij}(\vec{r})\,dV \quad i,j = 1,3. \tag{4}$$

Since FEA can directly compute strain energies in linear elastic models, the mechanical work (W) performed by the cell can be easily quantified. Standard finite element software (ABAQUS Inc., Providence, Rhode Island) was used in this study.

2.6. Cell migration

AHDFs were seeded on different hydrogels at 500 cells/cm^2 and incubated for 12 h at 37 °C prior to the experiment. Time-lapse phase images of the cells were recorded every 15 min for up to 75 min with a MetaMorph®-operated CoolSNAP™ HQ camera (Universal Imaging Corporation, Downingtown, PA) attached to a Nikon Diaphot-TMD inverted microscope fitted with a 37 °C stage incubator and a 10× objective lens. Migration speed was determined from the time-lapse images using MetaMorph®, which tracked the distance covered by the center of a cell nucleus over a period of 75 min. The following sample size was used: 10 cells/field × 3 fields/replicate × 3 replicates.

2.7. Cell proliferation

Unlike other cell functions, proliferation was measured over a period of 3 days. Initially, a starting cell density of 500 cells/cm^2 was maintained. However, this low cell density resulted in a loss of cell viability during extended (>24 h) periods of culture. Therefore, the initial cell density was increased to 6000 cells/cm^2. AHDFs seeded on the different hydrogel surfaces were allowed to proliferate for three days, with the FULL-DMEM being changed every 24 h. All samples were fixed with 2% glutaraldehyde and stained with 0.1% crystal violet in 200 mM boric acid (pH 8.0). Photomicrographs of the stained AHDFs were obtained using a Nikon SMX800 zoom stereomicroscope (Japan) with Spot RT camera attachment (Diagnostic Instruments, Sterling Heights, MI). One field per well that covered almost 90% of the surface area (with 3 wells per condition) was imaged and the cell number quantified using MetaMorph® software (Universal Imaging, Downington, PA).

2.8. Data analysis

The number of replicates for each experiment was adjusted according to the variance obtained. Data is expressed as mean ± standard deviation and evaluated for differences by ANOVA followed by Tukey post-hoc analysis. Differences were considered significant when $p < 0.05$.

3. Results and discussion

3.1. Cell stiffness and cytoskeleton structure

AHDFs were plated on hydrogels of different stiffness for 12 h, which was sufficient to allow maximal spreading. AFM, operated in the SMFM mode, was used for in situ measurement of AHDF modulus (an index of stiffness). During our measurement, two simultaneous forces were exerted on the cells; first, a sinusoidal drive signal applied to the x-piezo that induced a small oscillatory motion on the cell surface, and second, a normal force of ~ 2 nN to maintain tip contact with the cell surface. The normal indenting force was applied to the perinuclear region between the cell nucleus and cytoplasmic edge to ensure reproducibility of the stiffness measurement. The lateral deflection (response) amplitude of the cantilever was measured and plotted against drive amplitude, with the response amplitude found to be proportional to drive amplitude (Fig. 1A), indicating that there was no slip during the cell-tip contact. Assuming a Hertzian model for this SMFM set-up, the response amplitude has been previously shown to be inversely proportional to 2/3 power of the lateral modulus of the specimen [13]. Using this calibration, we found that cell stiffness was sensitive to substrate mechanics (Fig. 1B), where a ~5-fold increase in hydrogel moduli (from 95 to 4270 Pa) produced a ~150% increase in cell moduli, with the stiffness on the various hydrogels showing significant difference.

Since actin microfilaments underlie the cell membrane and span the entire cytoplasm, we looked to see whether the adaptation of cell stiffness to substrate mechanics was

the direct result of corresponding alterations in actin cytoskeleton arrangement. Since the average doubling time of these AHDFs is about 18–20 h, limiting the culture time of cells on hydrogels to 12 h ensured that there were no artifacts produced by cytoskeleton rearrangements during mitosis. Fig. 2 shows the confocal images of AHDFs which were stained for the actin cytoskeleton. From the figure we see that the cells plated on stiff (4270 Pa) hydrogels had linear, stretched arrays of actin microfilaments with uniform diameter, similar to that observed in tissue culture plastic. The cells on the hydrogels of intermediate stiffness (550 Pa) demonstrated microfilaments of irregular diameter, with buckling produced in a few of them (indicated by arrows). In addition, the F-actin filament density decreased, with some small bright spots appearing in the cytoplasm. As the hydrogel substrate got even softer (95 Pa), the cells demonstrated a serpentine F-actin array of low density where now most of the microfilaments showed buckling (indicated by arrows). Furthermore, the density of bright cytoplasmic spots increased greatly. Based on their appearance and location, we speculate that these bright spots are actually the severed ends of F-actin filaments.

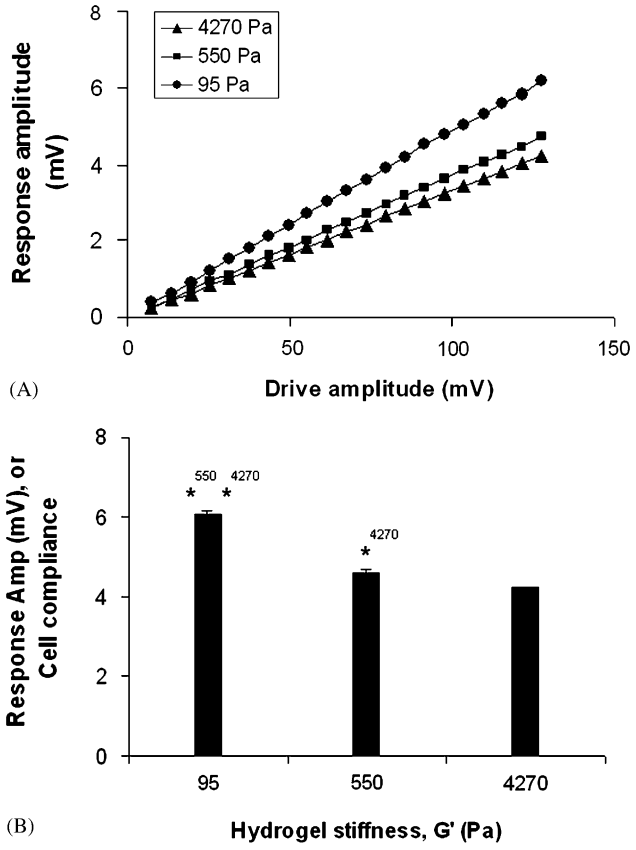

Fig. 1. Cell stiffness/compliance as a function of hydrogel mechanics. (A) The AFM response amplitude generated from cell's resistance to cantilever indentation increases linearly with the cantilever drive amplitude, which confirms the absence of any slip between the AFM tip and cell surface. The AFM was calibrated such that the smaller response amplitude corresponded to a stiffer surface and vice versa. (B) Response amplitude at drive amplitude of 120 mV is plotted against hydrogel mechanics, where cell stiffness increases with increasing substrate mechanics. * indicates $p<0.05$.

Similar effects of substrate mechanics on actin cytoskeleton assembly have been previously noted where NIH 3T3 fibroblasts demonstrated articulated stress fibers on stiff gels, which became diffuse when the cells were plated on soft gels [3]. Importantly, the increase in actin stretching on stiffer substrates also correlated well with an increase in AHDF stiffness observed on stiffer hydrogels. In fact, a similar relationship between actin assembly and cell stiffness has been previously shown in hepatocytes where disruption of F-actin bundles lowered both cell stiffness and spreading [16]. This group, like several others [17,18], also used AFM in contact mode to measure cell stiffness. In yet another and more detailed study, Wang et al. modulated the contractile state of human airway smooth muscle cells and utilized traction force microscopy and oscillatory magnetic twisting cytometry to show that cell prestress and stiffness are very closely associated [19].

Our findings provide additional and important experimental evidence in support of the tensegrity hypothesis by

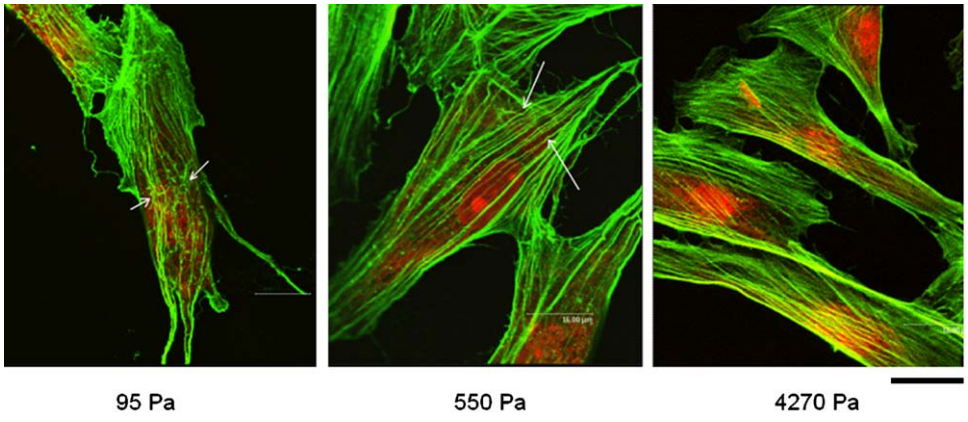

Fig. 2. Actin cytoskeleton organization on different hydrogels. Immunofluorescent staining with Alexa Flour 488-Phalloidin shows that actin fibers become more stretched and organized with increasing substrate mechanics. Arrows indicate areas of filament discontinuity and kinks/bucklings. Scale bar = 16 μm.

showing that a cell is hard-wired with an inter-connected, tension-bearing cytoskeleton network that senses substrate mechanics and undergoes rearrangement to reach a new equilibrium state. Both cell stiffness and cytoskeleton conformation depend on the level of isometric tension that, as we have shown, can be modulated by altering the substrate mechanics. Furthermore, many regulators of the biochemical machinery remain immobilized on the insoluble cytoskeleton [2,20]. Therefore, any change in cytoskeleton conformation is likely to affect its biophysical properties and, ultimately, intracellular physiology and cell function.

3.2. High-resolution detection of cellular traction

The intracellular contractile forces, which produce cytoskeleton tension and membrane stiffness, are exerted on the substrate as traction [10,21]. These cellular tractional forces have important implications in cell growth, migration and differentiation [22–24]. Determining their magnitude and localization would, therefore, allow one to predict and, perhaps, control cell fate. Since usually, cell traction cannot be measured directly, the typical procedure is to plate cells on micro-patterned or fluorescent bead-embedded elastic substrates, measure and map the traction-induced deformation using digital image processing techniques, and use elasticity theory to quantify tractional forces.

3.2.1. Measurement of cell-induced deformation using DISC

The DISC technique was used to measure the AHDF-generated deformation on the hydrogel surfaces with high spatial resolution and precision. 40 nm florescent beads were embedded in the hydrogels to produce speckles for the measurement of substrate deformation using DISC. Since the DISC matches the reference and deformed images subset by subset, possibilities of mismatch always exist, especially when the size of the subsets are small. To minimize uncertainty, a large subset is desired. On the other hand, since DISC calculates average displacement over the area of subset, the spatial resolution of DISC, which is critical for the traction force calculation, is determined by the size of subset and small subset is preferred for high spatial resolution. In fact, the accuracy and spatial resolution of DISC are determined by a combination of factors including size of subset, speckle size and density, image resolution and noise level. Ideally the speckles on an image should cover 50% of the image area and each speckle should have a size of 1.5–3.0 pixels in one dimension. To achieve 0.1 pixel accuracy and high spatial resolution, we chose to use a subset size that contained 3–9 speckles.

Once the AHDFs had adhered and spread on the hydrogel surfaces, digital images of the speckled hydrogels were acquired pre- and post-EDTA treatment, which caused cell detachment. The cellular traction exerted on the hydrogel surface was released following cell detachment, which resulted in bead displacement from the deformed to the original position. This slight deformation of the substrate can be detected precisely using DISC as shown in Fig. 3. The average magnitude of cell-induced deformation was typically greater on the softest (95 Pa) hydrogel than on the stiffest (4270 Pa) ones. This is perhaps because the 95 Pa hydrogel has much lower yield strength [9], where even small tractional forces causes large deformations. To clearly identify the magnitude and distribution of cellular traction on hydrogels of varying viscoelastic properties, we applied FEA to the displacement field obtained using DISC.

3.2.2. FEA

Previously, two approaches have been developed to calculate cellular traction forces, FTTC method and DW method, both of which were based on convolution theories [25,26]. Basically, these approaches begin with mapping a displacement field of the half space subjected to a (theoretical) unit force on surface. Then, a spectrum of forces is composed at various locations on the surface, either in real space with Monte Carlo method or in Fourier space, to reproduce the measured displacement field. These approaches are very computation intense; super computers are necessary for computation purposes.

Different from these reported deconvolution methods [25,26], FEA offers another straightforward approach to calculate cellular traction forces. Given the mechanical properties of the hydrogel substrate and complete boundary conditions, the traction forces can be easily computed by FEA using a simple linear elastic model of 3-D 8-node

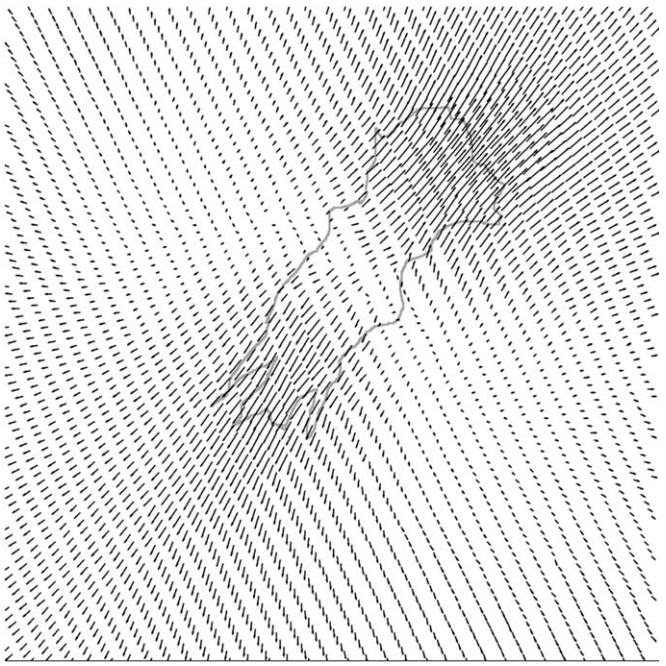

Fig. 3. DISC technique. A typical displacement field produced by a cell on a hydrogel substrate (4270 Pa). The actual displacement is very small; the magnitudes of all vectors have been amplified in this image for easier comprehension.

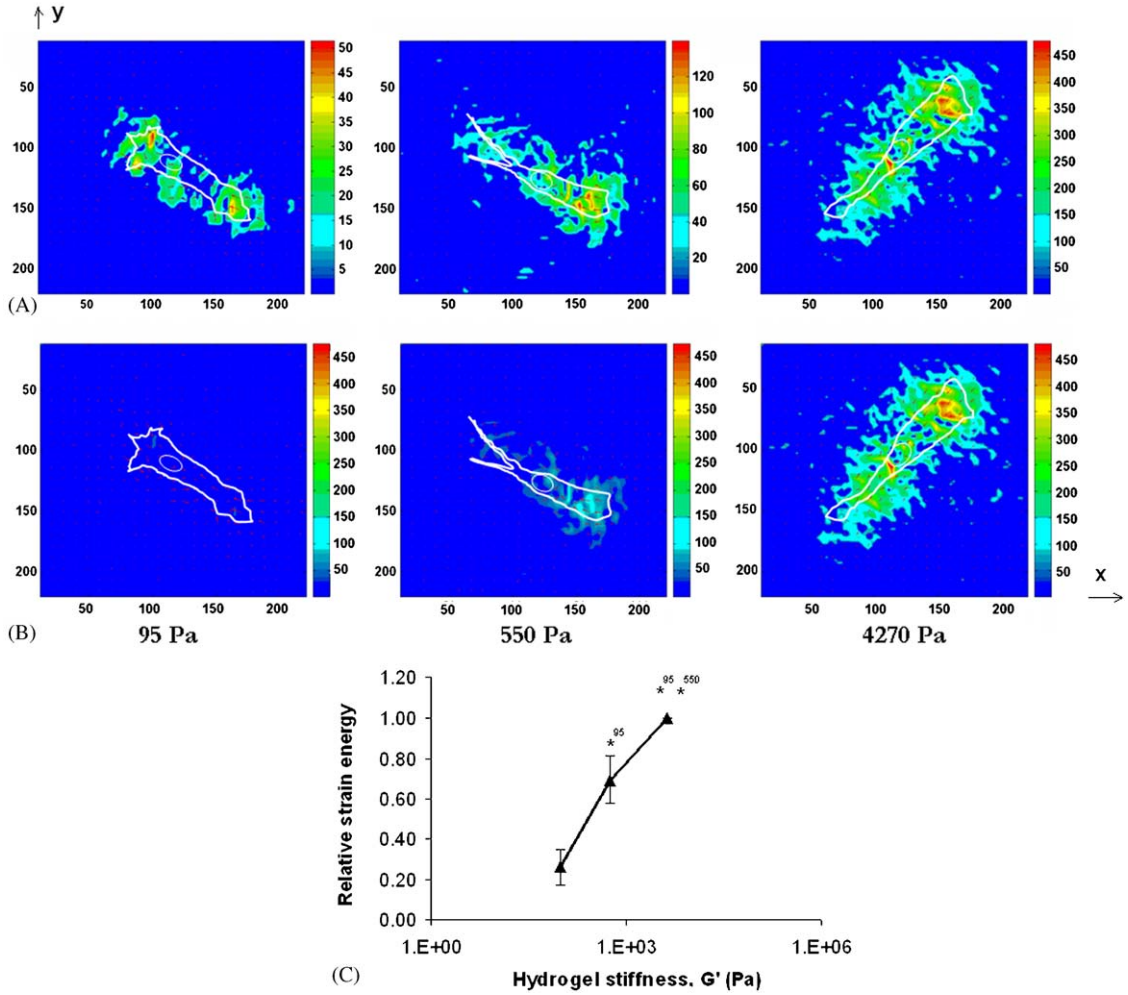

Fig. 4. Shear stress and strain energy using FEA. Cellular shear stresses (Pa) on the different hydrogels shown (A) on different scales, and (B) on one fixed scale. These stress maps were obtained by applying a FEA model on the displacement field that was obtained using DISC (Fig. 3). (C) Strain energy stored in the hydrogels as a result of the cellular mechanical work is plotted against hydrogel stiffness (absolute value for 4270 Pa hydrogels = 2.9 ± 0.1 pJ). * indicates $p < 0.05$.

brick elements. Contrary to the FTTC method, our approach does not require any Fourier transformation while unlike the DW method, both DISC and FEA deal with all the displacements and traction forces independent of the perceived cell boundary. Using our technique, the traction force vectors, including their magnitudes, directions and locations, can be precisely determined without specific staining of the focal adhesions. Because the Fredholm integral, which is traditionally involved in the calculation of traction forces from measured deformations, is avoided in our computations, both the stress field and the strain energy are calculated in a more straightforward manner. Compared with other computation intense algorithms that can only be implemented by super computers, FEA is a simpler approach to quantify not only the cellular traction forces but also the mechanical work done by the cell.

Fig. 4A shows the shear stress distribution calculated from the displacement field. The locations of the tractional forces are clearly visible in the maps. It can be seen that regardless of substrate viscoelasticity, the areas of strongest traction forces lie right behind the leading edges of the lamellipodia, which are known to be the regions containing focal adhesions that transmit cellular traction forces to the underlying substrate [27–29]. This indicates that our calculations based on FEA are reliable. Furthermore, on the stiff hydrogels, cells exerted stronger traction forces that were distributed along the cytoplasmic edge. On the contrary, cells on soft hydrogels exerted weaker traction forces, which appeared to be concentrated in smaller areas. The magnitude of traction stresses varied from 490 Pa on the stiff (4270 Pa) hydrogels to 140 and 50 Pa on the softer (550 and 95 Pa, respectively) ones. Therefore, the data shows a 3–4 fold increase in cellular traction with an approximately half-order increase in hydrogel mechanics, which is more apparent in Fig. 4B where the traction forces have all been plotted to the same scale.

The direction of tractional forces was largely orientated along the cell's axial direction. In some cases, the traction field was non-uniformly distributed at the two ends of the

cell, where the cell was subjected to stretching in both axial and trans-axial directions at the leading edge while only the axial direction at the trailing edge (data not shown). A similar observation has been previously reported [27], which is typical of a migrating cell where the lamellipodia at the leading edge explores every possible direction for migration while the posterior serves as an anchor to stabilize the whole cell until it is ready to detach from the substrate. Knowledge of this force distribution is essential in understanding the mechanism of the more complex en masse cell migration.

As a cell consolidates its focal adhesions on a substrate, it performs mechanical work, which is stored in the elastic substrate as strain energy and released upon cell detachment. Since active mechanosensing of substrate involves continuous formation and detachment of cell-matrix adhesions, we determined whether substrate mechanics influenced the cell's ability to perform work. As discussed earlier, work performed by cellular traction forces on various hydrogel substrates is assumed to be stored in the substrate as strain energy. Using FEA, we found that the strain energy on the stiff (4270 Pa) hydrogels was about 2.9 pJ, which decreased to 2.1 pJ on the 550 Pa hydrogels and to 0.81 pJ on the softest (95 Pa) hydrogels (Fig. 4C), with the differences being statistically significant. This trend in cellular work shows that cells can sense and respond to substrate mechanics by developing a feedback loop wherein the cell mechanics, which includes cytoskeleton tension (organization), cell stiffness and cellular traction, exists in dynamic equilibrium with substrate mechanics.

3.3. Cell functional responses

3.3.1. Cell migration

Cell migration is one of the most critical and physically integrated physiological processes that occur during embryogenesis, tissue morphogenesis and wound repair [21,30,31]. It requires a successful spatio–temporal coordination of several distinct cellular events such as membrane extension, formation of new adhesion complexes, generation of contractile force and traction and ultimately, rear release [21]. The intrinsic physical nature of this cell function suggests a strong correlation with cell and substrate mechanics.

Using time-lapse imaging and MetaMorph® software to analyze single-cell migration on different hydrogels, we found that the speed of AHDF migration decreased noticeably (>50%) with increasing substrate mechanics (Fig. 5A), with the average cell speed decreasing significantly from 0.81 μm/min on soft (95 Pa) hydrogels to 0.38 μm/min on the stiffest (4270 Pa) hydrogels. The high sensitivity of migration to substrate mechanics observed here is consistent with a previous study where cells migrated faster on soft polyacrylamide substrates and vice versa [26]. Additionally, from the phase-contrast time-lapse images, we found that cells on the softer hydrogels demonstrated dynamic lamellipodia activity, which was significantly reduced in cells on stiff hydrogels. Previous studies have shown a similar trend in lamellipodia ruffling as a function of substrate mechanics where a ~ 4-fold difference in gel moduli produced a ~ 6-fold difference in the rate of fluctuations in lamellipodia boundary [32]. The same group subsequently showed that the differences in lamellipodia activity corresponded to the observed differences in cell migration, which is consistent with our finding.

Our data shows that stiff substrates induce strong cellular traction (contractile) forces. In addition, we clearly show that the tractional force correlates inversely with cell migration speed, which is consistent with the established literature [28]. Importantly, an increase in cellular traction has been shown to induce growth of focal adhesion area [22], which is expected to simultaneously increase cell adhesion strength. Therefore, the decrease in cell migration speed with increasing traction force could perhaps be due to an increase in cell adhesiveness beyond the optimum level, as is observed with increasing adhesion strength through biological signaling [33].

3.3.2. Cell proliferation

The rate of cell proliferation has previously been shown to depend on the extent of cell spreading [34,35]. Since cell spreading may also dictate the amount of tractional force exerted by a cell [24], we investigated whether the magnitude of cellular traction directly affected cell

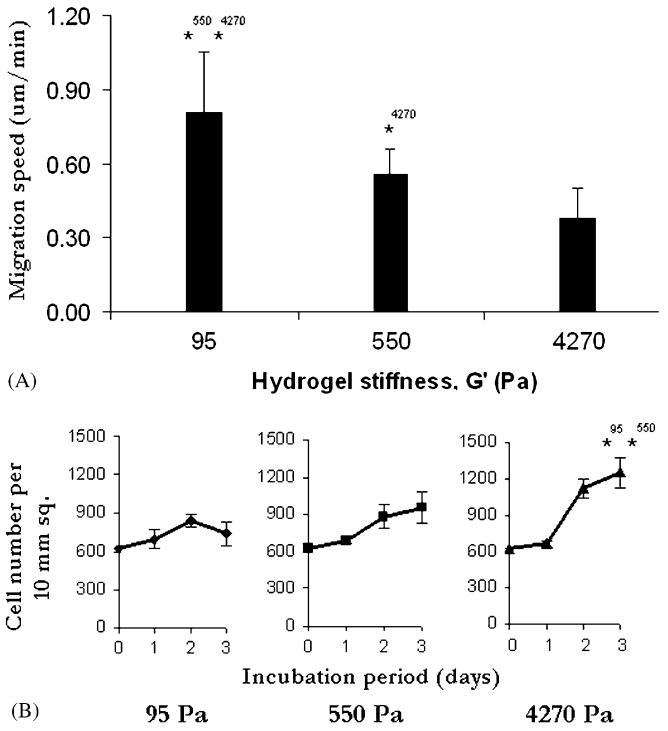

Fig. 5. (A) Single-cell migration. Migration speed decreases with increasing hydrogel stiffness; (B) Cell proliferation. Contrary to migration, cell proliferation increases with increasing hydrogel stiffness. Cell counting was performed using MetaMorph software. Day 3 cell count showed significant difference. * indicates $p<0.05$.

proliferation. AHDFs were allowed to proliferate on the different hydrogels for a period of 3 days. Fig. 5B shows that cell density on all hydrogels increased marginally by day 1, which is expected since the average doubling time for AHDFs is ~ 18–20 h. On day 2, however, there was a dramatic difference in cell density between the hydrogels. AHDFs proliferated normally only on the stiffest hydrogels, while their rate of proliferation was markedly reduced on softer hydrogels. By day 3, AHDF numbers increased significantly on the stiffest (4270 Pa) hydrogels, while those on the softest ones (95 Pa) actually underwent a decline, suggesting inhibition in cell adhesion or cell death or both. Since we earlier showed that AHDFs on soft hydrogels fail to exert strong tractional forces, our data shows that the magnitude of tractional forces exerted on the substrate may influence cell proliferation.

4. Conclusion

Taken together, our results present a comprehensive view of how cells adapt to substrate mechanics by adjusting their biophysical properties at the whole-cell level that eventually affect cell function. These findings necessitate the optimization of mechanical design parameters of engineered tissue constructs that are aimed at stimulating rapid and accentuated cell functional responses. The acellular, bioactive HA/FN hydrogels reported here have been designed to accentuate tissue repair. During wound repair, fibroblast migration into the initial fibrin/FN provisional matrix acts as the rate-limiting step in granulation tissue formation [36]. These migrating fibroblasts lyse the clot and lay down the second provisional matrix containing HA/FN that supports cell proliferation [37]. Once the invading fibroblasts have covered the entire wound space, they secrete collagen and undergo rapid proliferation. Importantly, both the HA and collagen matrices possesses greater viscoelastic strength than fibrin matrix. Therefore, the opposite effects of substrate mechanics on cell migration and proliferation observed in this report could, in part, explain why, during wound repair, fibroblasts migrate rapidly through the softer fibrin/FN clot and then proliferate rapidly within the stiffer HA/FN and collagen/FN matrices. Cues from our present findings are expected to guide the development of more robust tissue engineered constructs with strong conductive and inductive properties to facilitate tissue repair or induce tissue regeneration.

Acknowledgments

Financial support to R.A.F.C. (NIH Grant# AG010143), M.H.R. (NSF-MRSEC program and DOE) and X.-D.R (NIH Grant# AR47894) is gratefully acknowledged. The authors thank Drs. Glenn D. Prestwich and Xiao Zheng Shu (Department of Medicinal Chemistry, University of Utah) for providing thiol-derivatized HA and sharing the chemistry to obtain crosslinked HA hydrogels.

References

[1] Lutolf MP, Hubbell JA. Synthetic biomaterials as instructive extracellular microenvironments for morphogenesis in tissue engineering. Nat Biotechnol 2005;23:47–55.
[2] Discher DE, Janmey P, Wang YL. Tissue cells feel and respond to the stiffness of their substrate. Science 2005;310:1139–43.
[3] Georges PC, Janmey PA. Cell type-specific response to growth on soft materials. J Appl Physiol 2005;98:1547–53.
[4] Wang YL, Pelham Jr. RJ. Preparation of a flexible, porous polyacrylamide substrate for mechanical studies of cultured cells. Methods Enzymol 1998;298:489–96.
[5] Harris AK, Stopak D, Wild P. Fibroblast traction as a mechanism for collagen morphogenesis. Nature 1981;290:249–51.
[6] Hinz B, Celetta G, Tomasek JJ, Gabbiani G, Chaponnier C. Alpha-smooth muscle actin expression upregulates fibroblast contractile activity. Mol Biol Cell 2001;12:2730–41.
[7] Ghosh K, Ren XD, Shu XZ, Prestwich GD, Clark RA. Fibronectin functional domains coupled to hyaluronan stimulate adult human dermal fibroblast responses critical for wound healing. Tissue Eng 2006;12:601–13.
[8] Toole BP. Proteoglycans and hyaluronan in morphogenesis and differentiation. In: Hay ED, editor. Cell biology of the extracellular matrix. New York: Plenum Press; 1991.
[9] Ghosh K, Shu XZ, Mou R, Lombardi J, Prestwich GD, Rafailovich MH, et al. Rheological characterization of in situ cross-linkable hyaluronan hydrogels. Biomacromolecules 2005;6:2857–65.
[10] Huang S, Ingber DE. The structural and mechanical complexity of cell-growth control. Nat Cell Biol 1999;1:E131–8.
[11] Guan E, Smilow S, Rafailovich M, Sokolov J. Determining the mechanical properties of rat skin with digital image speckle correlation. Dermatology 2004;208:112–9.
[12] Kishimoto J, Ehama R, Ge Y, Kobayashi T, Nishiyama T, Detmar M, et al. In vivo detection of human vascular endothelial growth factor promoter activity in transgenic mouse skin [see comments]. Am J Pathol 2000;157:103–10.
[13] Zhang Y, Ge S, Rafailovich MH, Sokolov JC, Colby RH. Surface characterization of cross-linked elastomers by shear modulation force microscopy. Polymer 2003;44:3327–32.
[14] Bathe K. Finite element procedures. NJ: Prentice-Hall; 1996.
[15] Slaughter WS. The linearized theory of elasticity. New York: Birkhauser Boston; 2002.
[16] Bhadriraju K, Hansen LK. Extracellular matrix- and cytoskeleton-dependent changes in cell shape and stiffness. Exp Cell Res 2002;278:92–100.
[17] Rotsch C, Jacobson K, Radmacher M. Dimensional and mechanical dynamics of active and stable edges in motile fibroblasts investigated by using atomic force microscopy. Proc Natl Acad Sci USA 1999;96:921–6.
[18] Shroff SG, Saner DR, Lal R. Dynamic micromechanical properties of cultured rat atrial myocytes measured by atomic force microscopy. Am J Physiol 1995;269:C286–92.
[19] Wang N, Tolic-Norrelykke IM, Chen J, Mijailovich SM, Butler JP, Fredberg JJ, et al. Cell prestress. I. Stiffness and prestress are closely associated in adherent contractile cells. Am J Physiol Cell Physiol 2002;282:C606–16.
[20] Ingber DE. The riddle of morphogenesis: a question of solution chemistry or molecular cell engineering? Cell 1993;75:1249–52.
[21] Lauffenburger DA, Horwitz AF. Cell migration: a physically integrated molecular process. Cell 1996;84:359–69.
[22] Riveline D, Zamir E, Balaban NQ, Schwarz US, Ishizaki T, Narumiya S, et al. Focal contacts as mechanosensors: externally applied local mechanical force induces growth of focal contacts by an mDia1-dependent and ROCK-independent mechanism. J Cell Biol 2001;153:1175–86.

[23] Chen J, Fabry B, Schiffrin EL, Wang N. Twisting integrin receptors increases endothelin-1 gene expression in endothelial cells. Am J Physiol Cell Physiol 2001;280:C1475–84.
[24] Galbraith CG, Sheetz MP. Forces on adhesive contacts affect cell function. Curr Opin Cell Biol 1998;10:566–71.
[25] Butler JP, Tolic-Norrelykke IM, Fabry B, Fredberg JJ. Traction fields, moments, and strain energy that cells exert on their surroundings. Am J Physiol Cell Physiol 2002;282:C595–605.
[26] Lo CM, Wang HB, Dembo M, Wang YL. Cell movement is guided by the rigidity of the substrate. Biophys J 2000;79:144–52.
[27] Pelham Jr. RJ, Wang Y. High resolution detection of mechanical forces exerted by locomoting fibroblasts on the substrate. Mol Biol Cell 1999;10:935–45.
[28] Oliver T, Lee J, Jacobson K. Forces exerted by locomoting cells. Semin Cell Biol 1994;5:139–47.
[29] Harris AK, Wild P, Stopak D. Silicone rubber substrata: a new wrinkle in the study of cell locomotion. Science 1980;208:177–9.
[30] Juliano RL, Haskill S. Signal transduction from the extracellular matrix. J Cell Biol 1993;120:577–85.
[31] Montrucchio G, Lupia E, de Martino A, Battaglia E, Arese M, Tizzani A, et al. Nitric oxide mediates angiogenesis induced in vivo by platelet-activating factor and tumor necrosis factor-alpha. Am J Pathol 1997;151:557–63.
[32] Pelham Jr. RJ, Wang Y. Cell locomotion and focal adhesions are regulated by substrate flexibility. Proc Natl Acad Sci USA 1997;94:13661–5.
[33] DiMilla PA, Stone JA, Quinn JA, Albelda SM, Lauffenburger DA. Maximal migration of human smooth muscle cells on fibronectin and type IV collagen occurs at an intermediate attachment strength. J Cell Biol 1993;122:729–37.
[34] Chen CS, Mrksich M, Huang S, Whitesides GM, Ingber DE. Geometric control of cell life and death. Science 1997;276:1425–8.
[35] Folkman J, Moscona A. Role of cell shape in growth control. Nature 1978;273:345–9.
[36] McClain SA, Simon M, Jones E, Nandi A, Gailit JO, Tonnesen MG, et al. Mesenchymal cell activation is the rate-limiting step of granulation tissue induction. Am J Pathol 1996;149:1257–70.
[37] Clark RAF. Wound repair: overview and general considerations. In: Clark RAF, editor. Molecular and cellular biology of wound repair. New York: Plenum press; 1996. p. 3–50.